

## OPEN

# Prospective Comparison of the Imaging Value of $^{99m}\text{Tc}$ -MDP Bone Scan and $^{68}\text{Ga}$ -FAPI-04 PET/CT in Synovitis, Acne, Pustulosis, Hyperostosis, and Osteitis Syndrome

Tingting Xu, MD, \*†‡ Haoyuan Ding, MD, \*†‡ Dongmei Fan, MBBS, \*†‡ Qingxue Shu, MD, § Guangfu Liu, MBBS, \*†‡ Shumao Zhang, MD, \*†‡ and Yue Chen, MD \*†‡

**Purpose:** This study aimed to explore the imaging value of  $^{68}\text{Ga}$ -FAPI-04 PET/CT in synovitis, acne, pustulosis, hyperostosis, and osteitis (SAPHO) syndrome and compare it with that of  $^{99m}\text{Tc}$ -MDP bone scan.

**Methods:** Nineteen participants with SAPHO syndrome underwent  $^{68}\text{Ga}$ -FAPI-04 PET/CT and  $^{99m}\text{Tc}$ -MDP bone scan. Demographic data and clinical features were recorded, SAPHO imaging features were analyzed, and the osteoarticular lesion detection rate in both methods was calculated.

**Results:** This prospective study recruited 4 men and 15 women aged  $52.4 \pm 8.6$  years. The anterior chest wall was involved in all participants (100%). Palmoplantar pustulosis was the most common (36.8%) skin symptom.  $^{99m}\text{Tc}$ -MDP bone scan and  $^{68}\text{Ga}$ -FAPI-04 PET/CT together detected 84 osteoarticular lesions, of which 91.7% (77/84) were detected by the former and 96.4% (81/84) by the latter. Furthermore,  $^{68}\text{Ga}$ -FAPI-04 PET/CT detected 5 cases of knee and hip joint synovitis.

**Conclusions:**  $^{68}\text{Ga}$ -FAPI-04 PET/CT was more sensitive than  $^{99m}\text{Tc}$ -MDP bone scan when evaluating osteoarticular lesions in SAPHO syndrome and could also evaluate synovial lesions.  $^{68}\text{Ga}$ -FAPI-04 PET/CT could be a good imaging method for SAPHO syndrome but requires further verification in a more extensive research cohort.

**Key Words:**  $^{68}\text{Ga}$ -FAPI-04,  $^{99m}\text{Tc}$ -MDP, bone scan, PET/CT, SAPHO syndrome

(*Clin Nucl Med* 2023;48: 768–774)

Synovitis, acne, pustulosis, hyperostosis, and osteitis (SAPHO) syndrome is a rare chronic aseptic inflammatory disease that involves multiple organs, including the bones, joints, and skin.<sup>1</sup> Osteoarticular disorder is a characteristic feature of SAPHO syndrome and typically involves the anterior chest wall.<sup>2,3</sup> Palmoplantar pustulosis is among the most common cutaneous features of SAPHO syndrome, followed by severe acne and psoriasis vulgaris.<sup>4</sup> The high heterogeneity of the disease makes its diagnosis and management challenging, especially if presenting with bone and joint but no skin involvement.<sup>1,5</sup>

Radiography and CT are commonly used for osteoarticular lesions assessment in SAPHO syndrome.<sup>5</sup> However, these conventional imaging modalities often fail to detect early-stage lesions.<sup>6</sup> A whole-body bone scan is a practical first-line approach for systematically evaluating osteoarticular lesions in SAPHO syndrome.<sup>6</sup> It is highly sensitive and can detect potential lesions without clinical manifestations.<sup>1</sup> Besides, it can reduce unnecessary biopsies.<sup>7</sup>

Fibroblast activation protein (FAP) is a type II transmembrane serine protease expressed by activated fibroblasts.<sup>8</sup> Fibroblast activation protein inhibitors (FAPis) can specifically target and bind to FAP and could be used as probes to visualize FAP-expressing lesions when radiolabeled.<sup>9</sup>  $^{68}\text{Ga}$ -FAPI has been introduced for tumor imaging and has demonstrated promising results. However, FAP expression is not cancer-specific; it is overexpressed in tissue remodeling sites associated with inflammation, fibrosis, rheumatological diseases, atherosclerosis, and cardiac injury, among others.<sup>10,11</sup>  $^{68}\text{Ga}$ -FAPI PET has shown good application prospects in imaging benign bone, joint, or muscle diseases, including immunoglobulin G4-related disease,<sup>12,13</sup> polymyositis,<sup>14</sup> rheumatoid arthritis,<sup>15</sup> osteoarthritis,<sup>11,16,17</sup> bone cyst,<sup>18</sup> fracture,<sup>19</sup> myositis ossificans,<sup>20</sup> Schmorl node,<sup>21</sup> osteofibrous dysplasia,<sup>16,22</sup> intraosseous meningioma,<sup>23</sup> and bone tuberculous.<sup>24</sup> The histopathological features of SAPHO syndrome are nonspecific osteomyelitis with inflammatory cell infiltration and a healing process with osteosclerosis and bone marrow fibrosis.<sup>4,25,26</sup> Therefore, we hypothesized that it would be possible to use  $^{68}\text{Ga}$ -FAPI imaging for SAPHO syndrome. We recently reported  $^{68}\text{Ga}$ -FAPI-04 PET/CT imaging results in a woman with SAPHO syndrome, showing potential application prospects.<sup>27</sup> This study aimed to explore the imaging value of  $^{68}\text{Ga}$ -FAPI-04 PET/CT in SAPHO syndrome and compare it with that of  $^{99m}\text{Tc}$ -MDP bone scan.

## MATERIALS AND METHODS

### Study Design and Patients

Nineteen participants diagnosed with SAPHO syndrome at our hospital were consecutively recruited from September 2020 to August 2022. This study was approved by the ethics committee of our hospital (AHSWMU-2020-035). Written informed consent

Received for publication March 9, 2023; revision accepted May 5, 2023.

From the \*Department of Nuclear Medicine, The Affiliated Hospital of Southwest Medical University; †Nuclear Medicine and Molecular Imaging Key Laboratory of Sichuan Province; ‡Institute of Nuclear Medicine, Southwest Medical University; and §Department of Rheumatology and Immunology, The Affiliated Hospital of Southwest Medical University, Luzhou, Sichuan, People's Republic of China.

Conflicts of interest and sources of funding: The authors declare that they have no competing interests. This work was supported by the school-level scientific research project of the Southwest Medical University (grant 2021ZKQN066) and Luzhou Science and Technology Plan Project (2022-JYJ-118).

T.X., H.D., and D.F. contributed equally to this article and shared joint first authorship. S.Z. and Y.C. contributed equally to this article and shared joint corresponding authorship.

Author Contributions: T.X., H.D., and D.F. contributed to the study design, and T.X. wrote the manuscript. T.X., H.D., D.F., and Q.S. collected and analyzed the clinical data of patients. G.L. is responsible for image processing of all patients. S.Z. and Y.C. was responsible for revising for important intellectual content. S.Z. and Y.C. contributed equally to this article and shared joint corresponding authorship. All authors read and approved the final manuscript.

Correspondence to: Yue Chen, MD, Department of Nuclear Medicine, The Affiliated Hospital of Southwest Medical University, Nuclear Medicine and Molecular Imaging Key Laboratory of Sichuan Province, Institute of Nuclear Medicine, Southwest Medical University, No. 25 TaiPing St, Jiangyang District, Luzhou, Sichuan 646000, People's Republic of China. E-mail: chenye523@126.com; Shumao Zhang, MD, Department of Nuclear Medicine, The Affiliated Hospital of Southwest Medical University, Nuclear Medicine and Molecular Imaging Key Laboratory of Sichuan Province, Institute of Nuclear Medicine, Southwest Medical University, No. 25 TaiPing St, Jiangyang District, Luzhou, Sichuan 646000, People's Republic of China. E-mail: zhangshumao1127@126.com.

Copyright © 2023 The Author(s). Published by Wolters Kluwer Health, Inc. This is an open-access article distributed under the terms of the Creative Commons Attribution-Non Commercial-No Derivatives License 4.0 (CCBY-NC-ND), where it is permissible to download and share the work provided it is properly cited. The work cannot be changed in any way or used commercially without permission from the journal.

ISSN: 0363-9762/23/4809-0768

DOI: 10.1097/RLU.0000000000004752

was obtained from all participants. After enrollment, the participants underwent <sup>68</sup>Ga-FAPI-04 PET/CT and <sup>99m</sup>Tc-MDP bone scan within 1 week. The recorded demographic data and clinical features included age, sex, age at onset of dermatological and osteoarticular symptoms, age at SAPHO syndrome diagnosis, disease duration, and dermatological manifestations (palmoplantar pustulosis, severe acne, or psoriasis vulgaris). Laboratory evaluations included erythrocyte sedimentation rate (ESR), high-sensitivity C-reactive protein (hs-CRP), rheumatoid factor, antinuclear antibody (ANA), and human leukocyte antigen B27 (HLA-B27), measured within 1 week of the PET/CT examination. Findings in joint ultrasonography, CT, and MRI were recorded. Pathological skeletal involvement results, if any, were also recorded. All participants were followed up for at least 3 months. The <sup>68</sup>Ga-FAPI-04 PET/CT imaging results of 1 of the 19 participants were previously reported.<sup>27</sup>

### Diagnostic and Exclusion Criteria

The diagnostic criteria for SAPHO syndrome included (1) bone and joint involvement associated with palmoplantar pustulosis, psoriasis vulgaris, or severe acne; (2) isolated sterile hyperostosis/osteitis (adults); (3) chronic recurrent multifocal osteomyelitis (children); and (4) bone and joint involvement associated with chronic bowel diseases.<sup>28</sup> The exclusion criteria were septic osteomyelitis, infectious chest wall arthritis, bone tumor, diffuse idiopathic skeletal hyperostosis, osteoarticular manifestations of retinoid therapy, palmoplantar keratoderma, and infectious palmoplantar pustulosis.<sup>6,25</sup>

### <sup>99m</sup>Tc-MDP Bone Scan and <sup>68</sup>Ga-FAPI-04 PET/CT Imaging

Whole-body bone scan was performed 3 to 4 hours after intravenous injection of 740 to 925 MBq (20–25 mCi) <sup>99m</sup>Tc-MDP. SPECT/CT of the symptomatic sites and/or sites of abnormal uptake was performed. The injection dose of <sup>68</sup>Ga-FAPI-04 was 1.85 MBq (0.05 mCi)/kg. PET/CT scanning from head to foot (3 minutes per bed position) was performed 40 to 60 minutes after the tracer injection. The resulting images were corrected by attenuation and reconstructed iteratively to obtain the transverse, coronal, and sagittal views of the PET/CT scans.

### Image Analysis

All images were evaluated by 3 experienced nuclear medicine physicians blinded to the clinical features and laboratory evaluations. Interobserver differences in image interpretation were resolved by discussion, and a diagnostic consensus was reached. We defined several major regions to classify the lesion sites: anterior chest wall, comprising the ribs, sternoclavicular joints, costosternal joints, anterior first rib, clavicles, and sternum; axial skeleton, comprising the spine (cervical, thoracic, and lumbosacral) and sacroiliac joints; pelvis; peripheral joints and bones; and craniofacial bone. The site and number of osteoarticular lesions with abnormal tracer uptake on PET/CT or bone scan, abnormal CT findings, and SUV<sub>max</sub> of lesions with abnormal tracer uptake on PET/CT were recorded. The imaging features on PET/CT and bone scan were analyzed, and the osteoarticular lesion detection rates by the 2 methods were calculated.

### Statistical Analysis

Data analysis was performed using IBM SPSS Statistics for Macintosh, Version 26.0 (IBM Corp, Armonk, NY). Descriptive data are shown as mean ± SD, median (range), or number (%).

## RESULTS

### Demographic and Clinical Characteristics

Table 1 presents the demographic and clinical characteristics of the 19 participants. The 4 men and 15 women had a mean age of

52.4 ± 8.6 years. Anterior chest wall involvement occurred in all participants (100%); 68.4% had skin symptoms, with palmoplantar pustulosis being the most common (36.8%). The hs-CRP and ESR were elevated in most participants. No participant had a positive HLA-B27 test, but 6 had a positive ANA test. Four participants underwent bone biopsies. The histopathology results indicated fibrous tissue hyperplasia accompanied by lymphocyte and plasma cell infiltration, suggesting chronic nonspecific inflammation.

### Imaging Characteristics of <sup>99m</sup>Tc-MDP Bone Scan

Bone scan detected 77 osteoarticular lesions (Table 2) and showed that anterior chest wall involvement occurred in all participants (100%), involving 65 lesions. A bull's-head sign was seen in 31.6% of the participants (6/19).

### Imaging Characteristics of <sup>68</sup>Ga-FAPI-04 PET/CT

PET/CT detected 81 osteoarticular lesions (Table 2) and showed that anterior chest wall involvement occurred in all participants (100%), involving 64 lesions. The median SUV<sub>max</sub> of all lesions was 4.3. The main bone and joint involvement manifestations included hyperostosis, osteosclerosis, or osteolysis. PET/CT detected 5 synovial lesions in the knee and hip joints (Figs. 1 and 2). A right breast nodule with abnormal tracer uptake (Fig. 1) detected in one participant was confirmed as lobular carcinoma in situ via puncture.

### <sup>99m</sup>Tc-MDP Bone Scan and <sup>68</sup>Ga-FAPI-04 PET/CT Osteoarticular Lesion Detection Rates

Bone scan and PET/CT together detected 84 osteoarticular lesions. Anterior chest wall involvement was the most common, with 67 lesions detected. The lumbosacral spine was the second most frequent site, with 7 lesions detected in 4 participants. The

**TABLE 1.** Demographic and Clinical Features of the 19 Participants With SAPHO Syndrome

Demographic and Clinical Features (N = 19)	
Age, mean ± SD, y	52.4 ± 8.6
Sex, male/female, n	4/15
Age at symptom onset, mean ± SD, y	49.6 ± 8.0
Age at osteoarticular symptoms onset, mean ± SD, y	50.5 ± 8.2
Age at skin lesion onset, mean ± SD, y	49.9 ± 8.1
Disease duration, mean ± SD, mo	29.4 ± 14.5
Osteoarticular symptoms, n (%)	
Anterior chest pain	19 (100)
Spinal pain	2 (10.5)
Sacroiliac pain	3 (15.8)
Peripheral skeletal or joint pain	2 (10.5)
Craniofacial pain	1 (5.3)
Skin manifestations, n (%)	
Palmoplantar pustulosis	7 (36.8)
Severe acne	5 (26.3)
Psoriasis vulgaris	2 (10.5)
Laboratory examinations	
ESR, mean ± SD, mm/h	41.1 ± 21.4
hs-CRP, mean ± SD, mg/L	7.6 ± 5.2
Elevated ESR, n (%)	13 (68.4)
Elevated hs-CRP, n (%)	7 (36.8)
ANA-positive, n (%)	6 (31.6)
Rheumatoid factor-positive, n (%)	0
HLA-B27-positive, n (%)	0

**TABLE 2.** Osteoarticular Lesions Revealed by <sup>99m</sup>Tc-MDP Bone Scan and <sup>68</sup>Ga-FAPI-04 PET/CT in 19 Participants

Site	<sup>99m</sup> Tc-MDP Bone Scan		<sup>68</sup> Ga-FAPI-04 PET/CT			Bone Scan + PET/CT	
	Patients	Lesions	Patients	Lesions	SUV <sub>max</sub> Median (Range)	Patients	Lesions
Anterior chest wall	19	65	19	64	4.5 (1.5–8.7)	19	67
Cervical spine	1	1	1	2	3.8 (3.3–4.3)	1	2
Thoracic spine	0	0	1	1	2.1	1	1
Lumbosacral spine	2	5	4	7	3.8 (2.1–4.6)	4	7
Sacroiliac joint	3	3	3	3	4.5 (1.9–5.8)	3	3
Pelvis	1	1	1	1	2.6	1	1
Peripheral joint and bone	1	1	1	1	4.4	1	1
Craniofacial bone	1	1	2	2	4.1 (2.0–6.2)	2	2
Total	—	77	—	81	4.3 (1.5–8.7)	—	84

detection rates of bone scan and PET/CT were 91.7% (77/84) and 96.4% (81/84), respectively (Table 2).

**DISCUSSION**

Previous studies have shown that anterior chest wall involvement is most common in SAPHO syndrome and occurs in 60% to

95% of adult patients.<sup>3,6</sup> In this study, anterior chest wall involvement occurred in all participants, with a slightly higher prevalence than previously reported. The coexistence of osteolysis and osteosclerosis was the main structural change observed in CT, especially in the anterior chest wall area. Some researchers believe that the radiographic features of SAPHO syndrome differ according to

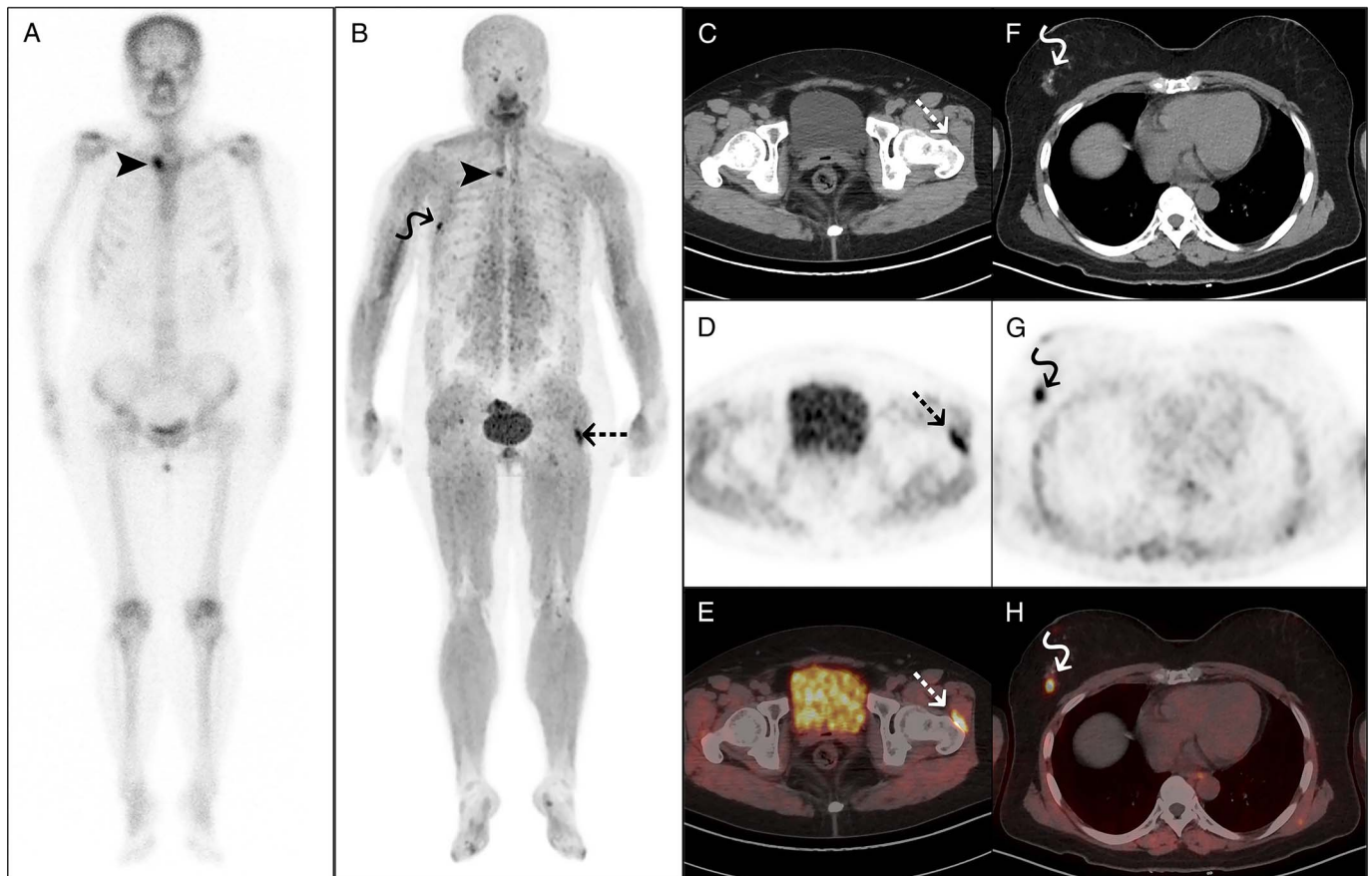


**FIGURE 1.** <sup>68</sup>Ga-FAPI-04 PET/CT detected left hip synovitis in a 57-year-old woman with SAPHO syndrome. The woman presented with anterior chest wall and left hip pain for 6 months and palmar pustules over the past 3 years. Laboratory examination showed elevated ESR (67 mm/h) and hs-CRP (13 mg/L) and a positive ANA test. <sup>99m</sup>Tc-MDP bone scan (A) and <sup>68</sup>Ga-FAPI-04 PET/CT (B) both showed increased tracer uptake in the right sternoclavicular joint (arrowheads). PET/CT (B–E) also showed increased tracer uptake in the synovial sac of the left hip joint (dotted arrows). Subsequent ultrasonography of the left hip confirmed the presence of synovitis. Furthermore, a nodule in the right breast with abnormal tracer uptake (F–H, curved arrows) was subsequently confirmed as lobular carcinoma in situ via puncture.

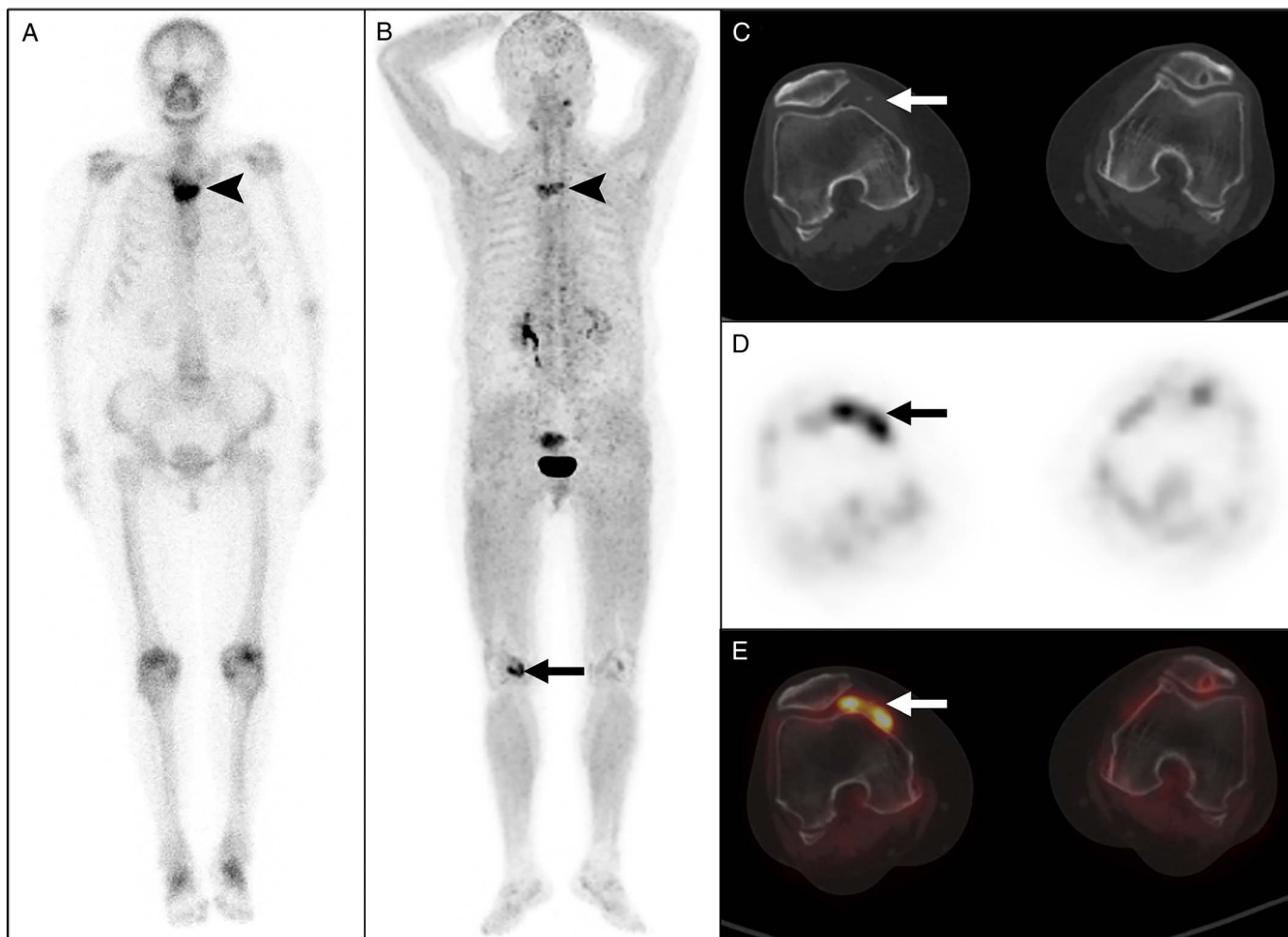


**FIGURE 2.**  $^{68}\text{Ga}$ -FAPi-04 PET/CT detected right knee synovitis in a 66-year-old woman with SAPHO syndrome. The woman presented with anterior chest wall pain for 5 months and multiple intermittent pustules in both feet over the past 2 years. No abnormality was found in the laboratory examination.  $^{99m}\text{Tc}$ -MDP bone scan (A) and  $^{68}\text{Ga}$ -FAPi-04 PET/CT (B) both showed increased tracer uptake in the sternal angle (arrowheads). PET/CT (B–E) also showed increased tracer uptake in the right knee joint (arrows). Subsequent ultrasonography of the right knee joint confirmed the presence of synovitis. A sternal biopsy showed signs of nonspecific chronic inflammation. This case was previously reported.<sup>27</sup>

the disease stage.<sup>6</sup> Early lesions tend to be osteodestructive, whereas later lesions tend to be osteoproliferative.<sup>6</sup>

Skin involvement is a typical manifestation of SAPHO syndrome. Previous studies found that most patients (94.9%) had dermatological manifestations,<sup>29</sup> and palmoplantar pustulosis was among the most common cutaneous features.<sup>6</sup> The incidence of skin involvement in our study (68.4%) was lower than previously reported.

The etiology of SAPHO syndrome remains elusive.<sup>2</sup> Two hypotheses were proposed to explain its possible pathogenesis.<sup>25</sup> One is that *Propionibacterium acnes* infection activates the innate immunity and T cell-mediated immune process.<sup>25</sup> The other hypothesis is the genetic theory, which suggests that SAPHO syndrome is possibly associated with HLA-B27.<sup>25</sup> However, some studies found no or only a few (2.5%–13%) HLA-B27-positive patients with SAPHO syndrome.<sup>2,29–31</sup> All participants in our study were negative for HLA-B27, suggesting that SAPHO syndrome may not be related to HLA-B27. The serum inflammatory markers hs-CRP and ESR were elevated in most participants, and 6 had a positive ANA test, suggesting that SAPHO syndrome was an inflammatory disease associated with autoimmunity.

Figures 3 and 4 show that  $^{68}\text{Ga}$ -FAPi-04 PET/CT detected more bone and joint lesions than  $^{99m}\text{Tc}$ -MDP bone scan, regardless of whether these lesions had significant density changes on CT. Our pilot study found that  $^{68}\text{Ga}$ -FAPi-04 PET/CT may be more sensitive than  $^{99m}\text{Tc}$ -MDP bone scan in detecting bone and joint lesions in SAPHO syndrome, even though it missed 3 anterior chest wall lesions in 2 participants (Fig. 4). Moreover,  $^{68}\text{Ga}$ -FAPi-04 PET/CT revealed knee and hip joint synovitis in 5 participants (Figs. 1 and 2), compensating for the limitation of  $^{99m}\text{Tc}$ -MDP bone scan in imaging soft tissue lesions. Dorst et al<sup>15</sup> found that arthritic joints of patients with rheumatoid arthritis showed clear  $^{68}\text{Ga}$ -FAPi-04 accumulation along the synovial membrane. Their *in vitro* experiments showed stable FAP gene expression in human synovial fibroblasts, indicating that inflamed synovium could be visualized using FAP-targeting tracers. Although there is no direct evidence to confirm the overexpression of FAP in bone joints or synovial lesions in our study, we speculate that  $^{68}\text{Ga}$ -FAPi-04 accumulation resulted from uptake by activated fibroblasts.

Moreover,  $^{68}\text{Ga}$ -FAPi-04 and  $^{99m}\text{Tc}$ -MDP are nonspecific tracers. Both might show abnormal uptake in various benign bone

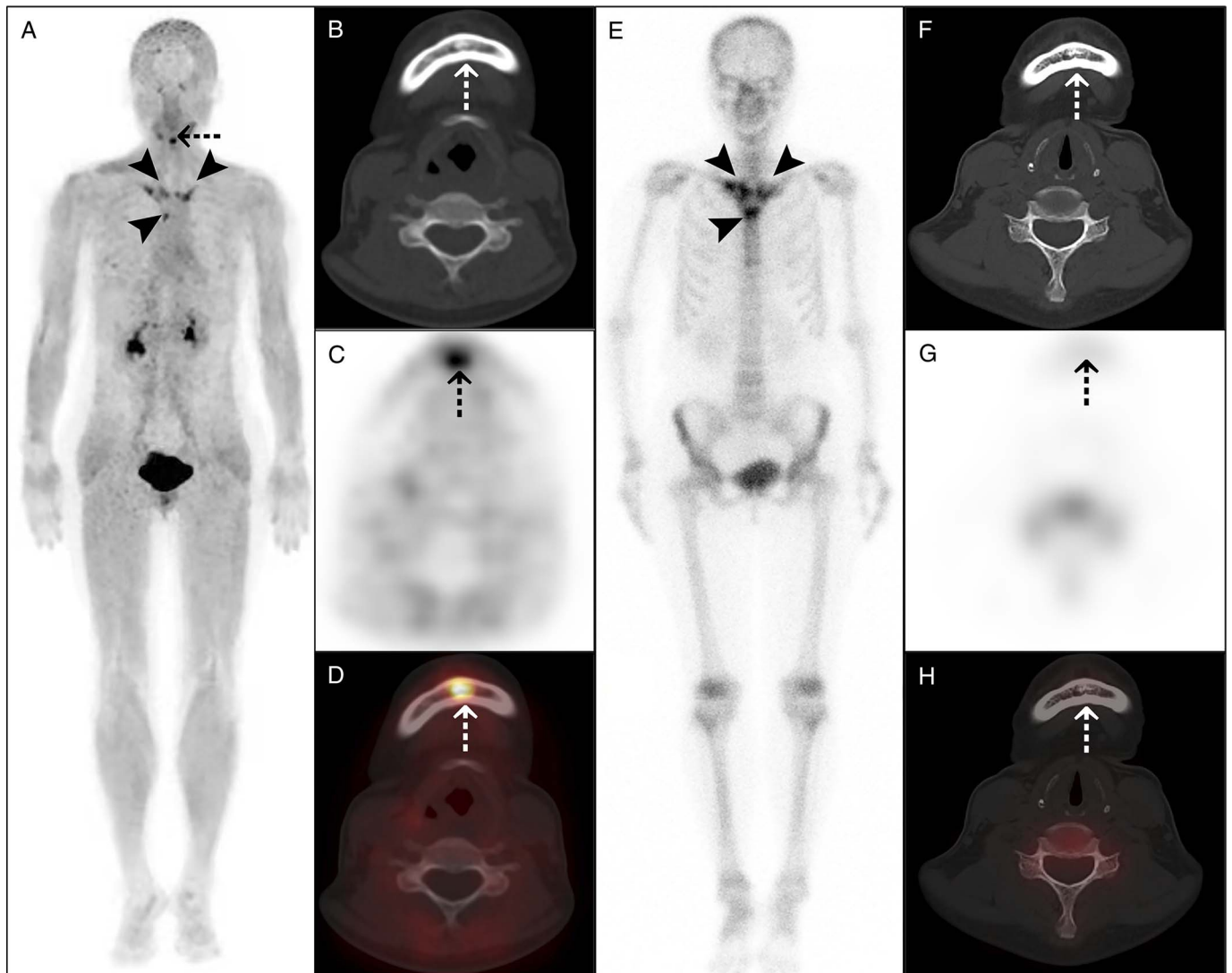


**FIGURE 3.**  $^{68}\text{Ga}$ -FAPI-04 PET/CT detected more osteoarticular lesions than  $^{99\text{m}}\text{Tc}$ -MDP bone scan in a 53-year-old woman with SAPHO syndrome. The woman presented with anterior chest wall pain for 3 years. Laboratory examination showed elevated ESR (32 mm/h) and a positive ANA test. The maximum intensity projection (A) of  $^{68}\text{Ga}$ -FAPI-04 PET/CT showed increased tracer uptake in the bilateral sternoclavicular joints, bilateral anterior first ribs, and sternal angle (arrowheads). Moreover, PET/CT (A–D) showed osteosclerosis in the mandible, with increased tracer uptake (dotted arrows).  $^{99\text{m}}\text{Tc}$ -MDP bone scan (E) showed increased tracer uptake in the above sites of anterior chest wall (arrowheads), resembling the bull's-head sign. However,  $^{99\text{m}}\text{Tc}$ -MDP bone scan showed no abnormal bone metabolism in the mandible (F–H, dotted arrows).

diseases, infectious diseases, and malignant bone tumors. SAPHO syndrome is often diagnosed after excluding other disease processes.<sup>6</sup> The bull's-head sign seen in whole-body bone scans is a characteristic feature of SAPHO syndrome.<sup>3</sup> In our study,  $^{99\text{m}}\text{Tc}$ -MDP bone scan showed the bull's-head sign in 31.6% (6/19) of the participants, higher than previously reported (10%–22.9%).<sup>6,29,32</sup> Because  $^{68}\text{Ga}$ -FAPI-04 PET/CT might not show the typical bull's-head sign seen in a whole-body bone scan, this reduces its diagnostic specificity. Moreover, some studies showed  $^{18}\text{F}$ -FDG could be used to distinguish active from inactive inflammatory lesions in SAPHO syndrome.<sup>33–36</sup>  $^{18}\text{F}$ -FDG PET/CT was not included in this study as it is not routinely used for this disease in clinical practice.

The limitations of this study include the following. First, the number of cases included was insufficient for a more detailed

statistical analysis. Second, biopsy results were available only for some participants, possibly introducing bias into our data. Third, this study did not evaluate the value of repetitive imaging in evaluating the curative effect because of the short follow-up and treatment heterogeneity. Fourth, no control group was included. A control group could help improve the interpretation of the SAPHO syndrome findings. This should be improved in future studies.

In summary,  $^{68}\text{Ga}$ -FAPI-04 PET/CT was a good evaluation approach for SAPHO syndrome. It was more sensitive than  $^{99\text{m}}\text{Tc}$ -MDP bone scan and could detect early-stage bone and joint lesions. It can also evaluate synovial lesions and assess the disease involvement more comprehensively than  $^{99\text{m}}\text{Tc}$ -MDP bone scan. However, these findings need to be verified in a larger research cohort.

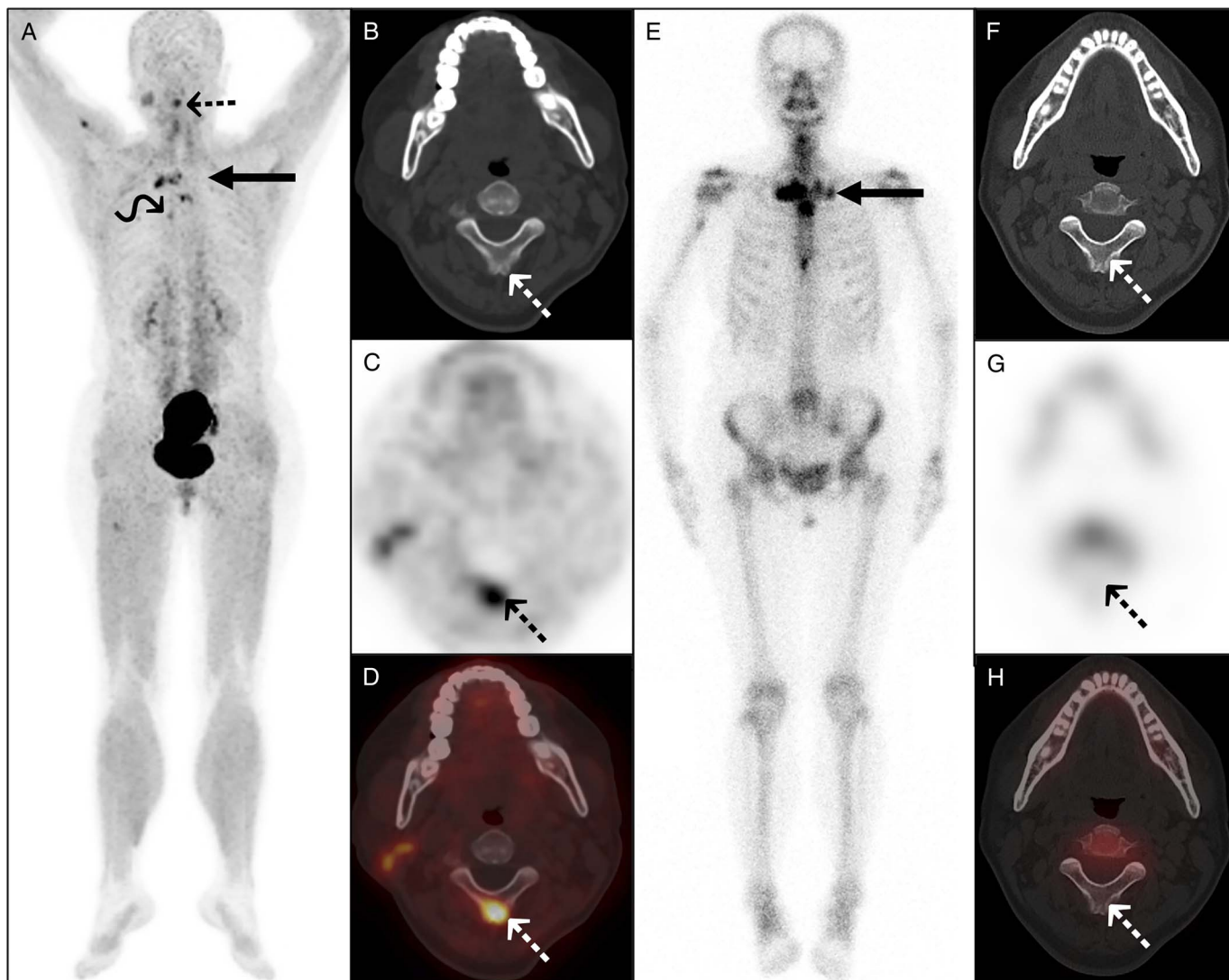


**FIGURE 4.** Complementarity of  $^{68}\text{Ga}$ -FAPI-04 PET/CT and  $^{99m}\text{Tc}$ -MDP bone scan in imaging a 52-year-old woman with SAPHO syndrome. The woman presented with facial acne for 3 years and whole-body bone pain for 1 year. Laboratory examination showed elevated ESR (48 mm/h) and hs-CRP (11.63 mg/L). The maximum intensity projection (A) of  $^{68}\text{Ga}$ -FAPI-04 PET/CT showed increased tracer uptake in the multiple bones and joints. Axial PET/CT (B–D) showed abnormal tracer uptake in the second cervical vertebra spinous process (dotted arrows), without apparent bone density changes. In contrast to PET/CT,  $^{99m}\text{Tc}$ -MDP bone scan additionally showed increased tracer uptake in the left sternoclavicular and sternocostal joints (E, long arrow), but not detected the lesions of the second cervical vertebra spinous process (F–H, dotted arrows) and the right sixth costal vertebra joint (curved arrow).

#### ACKNOWLEDGMENTS

The authors thank the members of the Department of Nuclear Medicine, The Affiliated Hospital, Southwest Medical University, and Nuclear Medicine and Molecular Imaging Key Laboratory of Sichuan Province, for their technical guidance, cooperation, and assistance in completing this study.

#### REFERENCES

- Shao S, Wang W, Qian Y. SAPHO syndrome involving the mandible treated with  $^{99m}\text{Tc}$ -MDP. *J Craniofac Surg*. 2020;31:510–512.
- Wang M, Li Y, Cao Y, et al. Mandibular involvement in SAPHO syndrome: a retrospective study. *Orphanet J Rare Dis*. 2020;15:312.
- Yu M, Cao Y, Li J, et al. Anterior chest wall in SAPHO syndrome: magnetic resonance imaging findings. *Arthritis Res Ther*. 2020;22:216.
- Sun X, Li C, Cao Y, et al. F-18 FDG PET/CT in 26 patients with SAPHO syndrome: a new vision of clinical and bone scintigraphy correlation. *J Orthop Surg Res*. 2018;13:120.
- Li C, Wang L, Wu N, et al. A retrospective study of bone scintigraphy in the follow-up of patients with synovitis, acne, pustulosis, hyperostosis, and osteitis syndrome: is it useful to repeat bone scintigraphy for disease assessment? *Clin Rheumatol*. 2020;39:1305–1314.
- Schaub S, Sirkis HM, Kay J. Imaging for synovitis, acne, pustulosis, hyperostosis, and osteitis (SAPHO) syndrome. *Rheum Dis Clin North Am*. 2016;42:695–710.
- Sallés M, Olivé A, Perez-Andres R, et al. The SAPHO syndrome: a clinical and imaging study. *Clin Rheumatol*. 2011;30:245–249.
- Backhaus P, Burg MC, Roll W, et al. Simultaneous FAPI PET/MRI targeting the fibroblast-activation protein for breast cancer. *Radiology*. 2022;302:39–47.

9. Qin C, Shao F, Gai Y, et al.  $^{68}\text{Ga}$ -DOTA-FAPI-04 PET/MR in the evaluation of gastric carcinomas: comparison with  $^{18}\text{F}$ -FDG PET/CT. *J Nucl Med*. 2022;63:81–88.
10. Giesel FL, Kratochwil C, Schlittenhardt J, et al. Head-to-head intra-individual comparison of biodistribution and tumor uptake of  $^{68}\text{Ga}$ -FAPI and  $^{18}\text{F}$ -FDG PET/CT in cancer patients. *Eur J Nucl Med Mol Imaging*. 2021;48:4377–4385.
11. Erol Fenercioglu Ö, Beyhan E, Ergül N, et al.  $^{18}\text{F}$ -FDG PET/CT and  $^{68}\text{Ga}$ -FAPI-4 PET/CT findings of bilateral knee osteoarthritis in a patient with uveal malignant melanoma. *Clin Nucl Med*. 2022;47:e144–e146.
12. Pan Q, Luo Y, Zhang W. Recurrent immunoglobulin G4-related disease shown on  $^{18}\text{F}$ -FDG and  $^{68}\text{Ga}$ -FAPI PET/CT. *Clin Nucl Med*. 2020;45:312–313.
13. Luo Y, Pan Q, Yang H, et al. Fibroblast activation protein–targeted PET/CT with  $^{68}\text{Ga}$ -FAPI for imaging IgG4-related disease: comparison to  $^{18}\text{F}$ -FDG PET/CT. *J Nucl Med*. 2021;62:266–271.
14. Zheng J, Chen H, Lin K, et al. [ $^{68}\text{Ga}$ ][Ga-FAPI [ $^{18}\text{F}$ ]]FDG PET/CT images in a patient with juvenile polymyositis. *Eur J Nucl Med Mol Imaging*. 2021;48:2051–2052.
15. Dorst DN, Rijpkema M, Buitinga M, et al. Targeting of fibroblast activation protein in rheumatoid arthritis patients: imaging and ex vivo photodynamic therapy. *Rheumatology*. 2022;61:2999–3009.
16. Qin C, Song Y, Liu X, et al. Increased uptake of  $^{68}\text{Ga}$ -DOTA-FAPI-04 in bones and joints: metastases and beyond. *Eur J Nucl Med Mol Imaging*. 2022;49:709–720.
17. Xu T, Zhao Y, Ding H, et al. [ $^{68}\text{Ga}$ ][Ga-DOTA-FAPI-04 PET/CT imaging in a case of prostate cancer with shoulder arthritis. *Eur J Nucl Med Mol Imaging*. 2021;48:1254–1255.
18. Gungor S, Selcuk NA. Benign bone cyst mimicking bone metastasis demonstrated on  $^{68}\text{Ga}$ -FAPI. *Clin Nucl Med*. 2022;47:e95–e97.
19. Lv Y, Lan X, Qin C. Incidental detection of sacral insufficiency fracture on  $^{68}\text{Ga}$ -FAPI PET/MR. *Clin Nucl Med*. 2021;46:1032–1033.
20. Gong W, Chen S, He L, et al. Intense  $^{68}\text{Ga}$ -FAPI uptake in a patient with myositis ossificans: mimicking bone malignancy. *Clin Nucl Med*. 2022;47:638–639.
21. Wu J, Tang W, Wang Y, et al. Schmorl node can cause increased  $^{68}\text{Ga}$ -FAPI activity on PET/CT. *Clin Nucl Med*. 2022;47:537–538.
22. Wang Y, Wu J, Liu L, et al.  $^{68}\text{Ga}$ -FAPI-04 PET/CT imaging for fibrous dysplasia of the bone. *Clin Nucl Med*. 2022;47:e9–e10.
23. Gong W, Yang X, Li L, et al. Elevated  $^{68}\text{Ga}$ -FAPI uptake by primary benign intraosseous meningioma. *Clin Nucl Med*. 2022;47:994–995.
24. Gong W, Yang X, Mou C, et al. Bone tuberculous granulomatous inflammation mimicking malignancy on  $^{68}\text{Ga}$ -FAPI PET/CT. *Clin Nucl Med*. 2022;47:348–349.
25. Gao S, Deng X, Zhang L, et al. The comparison analysis of clinical and radiological features in SAPHO syndrome. *Clin Rheumatol*. 2021;40:349–357.
26. Inoue K, Yamaguchi T, Ozawa H, et al. Diagnosing active inflammation in the SAPHO syndrome using  $^{18}\text{F}$ -FDG-PET/CT in suspected metastatic vertebral bone tumors. *Ann Nucl Med*. 2007;21:477–580.
27. Xu T, Huang Y, Zhao Y, et al.  $^{68}\text{Ga}$ -DOTA-FAPI-04 PET/CT imaging in a case of SAPHO syndrome. *Clin Nucl Med*. 2022;47:246–248.
28. Govoni M, Colina M, Massara A, et al. SAPHO syndrome and infections. *Autoimmun Rev*. 2009;8:256–259.
29. Cao Y, Li C, Yang Q, et al. Three patterns of osteoarticular involvement in SAPHO syndrome: a cluster analysis based on whole body bone scintigraphy of 157 patients. *Rheumatology*. 2019;58:1047–1055.
30. Aljuhani F, Toumadre A, Tatar Z, et al. The SAPHO syndrome: a single-center study of 41 adult patients. *J Rheumatol*. 2015;42:329–334.
31. Cianci F, Zoli A, Gremese E, et al. Clinical heterogeneity of SAPHO syndrome: challenging diagnose and treatment. *Clin Rheumatol*. 2017;36:2151–2158.
32. Fu Z, Liu M, Li Z, et al. Is the bullhead sign on bone scintigraphy really common in the patient with SAPHO syndrome? A single-center study of a 16-year experience. *Nucl Med Commun*. 2016;37:387–392.
33. McGauvran AM, Kotsenas AL, Diehn FE, et al. SAPHO syndrome: imaging findings of vertebral involvement. *AJNR Am J Neuroradiol*. 2016;37:1567–1572.
34. Dong A, Bai Y, Cui Y, et al. FDG PET/CT in early and late stages of SAPHO syndrome: two case reports with MRI and bone scintigraphy correlation. *Clin Nucl Med*. 2016;41:e211–e215.
35. Pichler R, Weiglein K, Schmekal B, et al. Bone scintigraphy using Tc-99m DPD and F18-FDG in a patient with SAPHO syndrome. *Scand J Rheumatol*. 2003;32:58–60.
36. Kohlfuerst S, Igerc I, Lind P. FDG PET helpful for diagnosing SAPHO syndrome. *Clin Nucl Med*. 2003;28:838–839.